HHS Public Access

Author manuscript

*Exp Eye Res*. Author manuscript; available in PMC 2019 November 01.

Published in final edited form as:

*Exp Eye Res*. 2018 November ; 176: 243–251. doi:10.1016/j.exer.2018.09.002.

# NOD and NOR mice exhibit comparable development of lacrimal gland secretory dysfunction but NOD mice have more severe autoimmune dacryoadenitis

**Yaping Ju**[1], **Srikanth Reddy Janga**[2], **Wannita Klinngam**[1], **J. Andrew MacKay**[1], **Dillon Hawley**[3], **Driss Zoukhri**[3], **Maria C. Edman**[2], and **Sarah F. Hamm-Alvarez**[1,2,*]

[1]Department of Pharmacology and Pharmaceutical Sciences, School of Pharmacy, University of Southern California, Los Angeles, California, United States

[2]Department of Ophthalmology, Roski Eye Institute, Keck School of Medicine, University of Southern California, Los Angeles, California, United States

[3]Department of Comprehensive Care, Tufts University School of Dental Medicine, Boston, Massachusetts, United States

## Abstract

The male Non-Obese Diabetic (NOD) mouse is an established model of autoimmune dacryoadenitis characteristic of Sjögren's Syndrome (SS), but development of diabetes may complicate studies. The Non-Obese Diabetes Resistant (NOR) mouse is a MHC-II matched diabetes-resistant alternative, but development of autoimmune dacryoadenitis is not well-characterized. We compare features of SS in male NOD and NOR mice at 12 and 20 weeks. Stimulated tear secretion was decreased in 12 week NOD relative to BALB/c mice ($p<0.05$), while by 20 weeks both NOD and NOR showed decreased stimulated tear secretion relative to BALB/c mice ($p<0.001$). Tear CTSS activity was elevated in NOD and NOR relative to BALB/c mice ($p<0.05$) at 12 and 20 weeks. While NOD and NOR lacrimal glands (LG) showed increased LG lymphocytic infiltration at 12 and 20 weeks relative to BALB/c mouse LG ($p<0.05$), the percentage in NOD was higher relative to NOR at each age ($p<0.05$). Gene expression of CTSS, MHC II and IFN-γ in LG were significantly increased in NOD but not NOR relative to BALB/c at 12 and 20 weeks. Redistribution of the secretory effector, Rab3D in acinar cells was observed at both time points in NOD and NOR, but thinning of myoepithelial cells at 12 weeks in NOD and NOR mice was restored by 20 weeks in NOR mice. NOD and NOR mice share features of SS-like autoimmune dacryoadenitis, suggesting common disease etiology. Other findings suggest more pronounced lymphocytic infiltration in NOD mouse LG including increased pro-inflammatory factors that may be unique to this model.

*Address Correspondence to: Sarah F. Hamm-Alvarez, Ph. D., Department of Ophthalmology, 1450 San Pablo St., Room 4900, Mail Code 6103, Los Angeles CA 90033-6103, Tel: 323-442-1445, Fax: 323-442-6412.

Conflict of Interest

The authors declare no conflicting interests.

## 1. Introduction

Sjögren's syndrome (SS) is a systemic inflammatory autoimmune disease affecting more than 4 million Americans, and is characterized by lymphocytic infiltration of lacrimal glands (LG) and salivary glands (SG), reducing tear and saliva production and in severe cases, causing corneal damage and compromised oral health (Lemp, 2005; Maciel et al., 2016). The hallmark clinical symptoms of SS are persistent dry eye and mouth. In addition to exocrine gland dysfunction, SS patients progressively experience weight loss, fatigue, systemic inflammation of internal organs, and, in 5% of patients, B-cell lymphoma (Nocturne and Mariette, 2015; Routsias et al., 2013). Although first described by the Swedish ophthalmologist Henrik Sjögren in 1933 over 80 years ago, the pathological mechanisms and etiology of the disease are still not fully understood. Due to the lack of universally accepted diagnostic standards and specific disease markers, early diagnosis of SS is challenging, which makes it difficult to study the initiating biochemical and immunological events that occur prior to manifestation of the hallmark clinical symptoms. In this regard, mouse models are invaluable tools to understand disease pathogenesis as well as to develop promising new therapies.

Over the past decades, several spontaneous and experimentally induced mouse models of SS have been studied which have contributed significantly to our current understanding of the disease. One of the more extensively studied SS mouse models is the Non-Obese Diabetic mouse (NOD). NOD mice are derived from the outbred Jcl:ICR line of mice and are prone to developing a series of autoimmune syndromes including type 1 diabetes, autoimmune thyroiditis and autoimmune peripheral polyneuropathy (Many et al., 1996; Salomon et al., 2001). Furthermore, they spontaneously develop lymphocytic infiltration into the exocrine and endocrine glands (Hu et al., 1992; Humphreys-Beher, 1996) including the LG which is considered to be related to breakdown of multiple immune tolerance pathways (Anderson and Bluestone, 2005; Nguyen and Peck, 2009). Interestingly, male NOD mice exhibit a more severe LG disease as early as 8 weeks, possibly related to sex steroids (Takahashi et al., 1997), while the female NOD mice exhibit profound SG infiltration with lesser infiltration of LG (Roescher et al., 2012).

The NOD mouse shares many disease characteristics with human SS with respect to manifestations of disease. At the functional and tissue level, the LG of these mice and SS patients are infiltrated with T and B lymphocytes as well as other immune cells, while tear flow is reduced (Kikutani and Makino, 1992; Tsubota et al., 2000). Common mechanistic pathologies are also shared by these mice and SS patients associated with acinar secretory dysfunction. We have identified elevated cathepsin S (CTSS), a cysteine endopeptidase implicated in autoimmunity (Conus and Simon, 2010; Reddy et al., 1995), in lysosomes and secretory vesicle-like organelles in LG acinar cells in parallel with increased CTSS activity in tears of male NOD mice (Li et al., 2010). Increased tear CTSS activity is also detected in female SS patients relative to healthy controls, patients with non-autoimmune dry eye and patients with other autoimmune diseases (Hamm-Alvarez et al., 2014). A similar reduction in the expression and a redistribution to the basolateral domain of the exocytosis effector, Rab3D, has been observed in acinar cells from SS patients (Bahamondes et al., 2011) and male NOD mice (Meng et al., 2016). Atrophic myoepithelial cells (MEC), multipolar

stellate cells responsible for contraction to facilitate compression of acini to assist in expulsion of tears and saliva, and are detected by their enrichment in α-smooth muscle actin (SMA), are reduced in SS patients SG (Sisto et al., 2018) and in female NOD mice SG (Nashida et al., 2013). These findings suggest that NOD mice recapitulate characteristics of SS patients.

The incidence of spontaneous diabetes in the NOD mouse is 60% to 80% in females and 20% to 30% in males (Bach, 1994; Kikutani and Makino, 1992). Diabetes onset typically occurs from 12 to 14 weeks of age in female mice and later in male mice. Previously, we have used male NOD mice aged below 20 weeks, when most mice are diabetes free, in studies of SS disease biology as well as in development of potential SS therapeutics (Shah et al., 2017). However, the onset of diabetes may constitute a confounding factor for prolonged drug studies on autoimmune dacryoadenitis in male NOD mice. The Non-Obese Diabetes-Resistant (NOR) mice are a diabetes-free major histocompatibility II (MHC II)-matched alternative to the NOD mice. The NOR strain is the result of a genetic contamination of NOD with C57BL/KsJ. The C57BL/KsJ-derived non MHC-linked diabetes resistance factors in the NOR mice are reported not to affect the T-lymphocyte accumulation characteristics of NOD mice. Although, NOR mice have been used in a few studies of SS disease biology (Aluri et al., 2015; Aluri et al., 2017), there has not been a side-by-side characterization of NOR mice relative to NOD mice as models for SS-associated dacryoadenitis and other features of the disease process in the LG. Here we have compared the development and progression of SS-like ocular symptoms in male NOD and NOR mice relative to BALB/c healthy controls to provide an additional reference for mouse model selection for SS studies related to LG dysfunction. Comparison of the features that are shared between models to those that are distinct may also aid in understanding mechanisms responsible for development of these signs of SS.

## 2. Materials and Methods

### 2.1. Mice.

Male BALB/cJ (00065), NOD/ShiLtJ (001976) and NOR/LtJ (002050) mice were purchased from The Jackson Laboratory (Bar Harbor, ME, USA). All animal use was in compliance with policies approved by the University of Southern California Institutional Animal Care and Use Committee and experiments were conducted in accordance with the ARVO Statement for the Use of Animals in Ophthalmic and Vision Research.

### 2.2. Reagents.

The rabbit anti-CTSS polyclonal antibody (Catalog No. 6686–100) and the CTSS activity assay kit were from Biovision (Milpitas, CA, USA). Rabbit anti-Rab3D polyclonal antibody was generated by Antibodies Inc. (Davis, CA) as previously reported (Evans et al., 2008). Polyclonal rabbit anti-SMA antibody (Catalog No. ab5694) was from Abcam (Cambridge, UK). Bovine serum albumin was from Jackson ImmunoResearch Laboratories (Westgrove, PA, USA). Rhodamine phalloidin, Alexa-Fluor 488 goat anti-rabbit secondary antibody and ProLong Gold Antifade Mounting Medium were from Invitrogen (Carlsbad, CA, USA). Ketamine (Ketaject) was from Phoenix (St. Joseph, MO, USA) and xylazine (AnaSed) was

from Akorn (Lake Forest, IL, USA). Carbachol, used to stimulate tear production, was from Sigma-Aldrich (St. Louis, MO, USA). O.C.T. Compound was obtained from Sakura Lifetek (Torrance, CA, USA). The reverse transcription kit, TaqMan Universal PCR Master Mix, and primers for realtime (RT)-PCR analysis of GAPDH (glyceraldehyde 3-phosphate dehydrogenase Mm99999915_g1), CTSS (Mm01255859_m1), MHC II (Mm00439216_m1) and interferon-γ (IFN-γ) (Mm00801778_m1) were from Life Technologies (Grand Island, NY, USA). The RNeasy plus Universal Mini Kit was from Qiagen (Valencia, CA, USA). ZoneQuick phenol red threads were purchased from SHOWA YAKUHIN KAKO CO., LTD (Tokyo, Japan). Free Style Lite test strips were from Abbott Diabetes Care, Inc. (Alameda, CA, USA). The Bio-Rad protein assay kit was from Bio-Rad (Hercules, CA, USA). All other chemicals were reagent grade and obtained from standard suppliers.

### 2.3. Blood Glucose Measurements.

Mice were anesthetized briefly using a continuous flow of isoflurane through a nose cone. A tail nick was made and a drop of peripheral blood was collected. Blood glucose was measured using the Free Style Lite test strips read with a glucose meter (Abbott Diabetes Care, Inc., Alameda, CA, USA).

### 2.4. Basal and Stimulated Tear Measurements.

Basal and stimulated tears were measured as described (Shah et al., 2013; Shah et al., 2017). Briefly, for measurement of basal tear flow, a ZoneQuick phenol red impregnated cotton thread was inserted under the lower eyelid for 10 sec while mice were under anesthesia, and tear production was reported as a function of the length of wetting of the thread in millimeters. The procedure was repeated in each eye and data presented are an average of the wetting length of the threads from both eyes. For collection of stimulated tear fluid, a small incision was made to expose the LG of anesthetized mice. A small piece of cellulose mesh (Kimwipe; Fisher Scientific, Pittsburgh, PA, USA) was placed on the LG to capture added secretagogue (3 μl of 50 μM carbachol solution). After stimulating the gland for 5 min, tears from both eyes were collected with 2 μl microcapillary tubes (Drummond Scientific, Broomall, PA, USA.) Stimulation was performed three times for a total collection time of 15 min, and the volume of collected tears was recorded. Tears were placed on ice until further biochemical analysis.

### 2.5. CTSS Activity Analysis.

CTSS activity in tears was measured using a protocol modified from that described previously (Hamm-Alvarez et al., 2014; Li et al., 2010). Briefly, stimulated mouse tear fluid was diluted in 200 μL of CTSS reaction buffer and divided into two 100 μL reactions on a 96-well plate. A CTSS–specific inhibitor was added to one of the two wells for each sample. After incubation at 37 °C for 1 hour, the plate was read using a SpectraMax Gemini EM Microplate Reader with emission at 400nm and excitation at 505 nm. After the experiment, the Bio-Rad protein assay was performed per the manufacturer's protocol and CTSS activity was normalized to 1 μg total tear protein.

### 2.6. Real-Time PCR.

For measurement of gene expression, total RNA was isolated from whole LG using the RNeasy plus Universal Mini Kit per the manufacturer's protocol. DNA was prepared using the reverse transcription kit per the manufacturer's recommendations. Quantitative (real-time) PCR was performed with the TaqMan gene expression assays on the ABI 7900HT real-time PCR system, using the following probes: IFN-γ, MHC II, and CTSS. GAPDH was used as a control housekeeping gene. Each reaction consisted of 1 μL cDNA from the reverse transcription reaction mixed with 8 μL nuclease-free water and 1 μL assay primer mixed with 10 μL TaqMan Universal PCR Master Mix. Each sample was run in triplicate. The thermal profile consisted of preheating the samples at 95.8°C for 10 min followed by 40 repeats at 95.8°C for 15 sec each and 60.8°C for 1 min. The relative expression levels were calculated using the comparative CT method (ΔΔCT method) on the default ABI software SDS 2.3 (ThermoFisher Scientific, Waltham, MA, USA), as described previously (Wu et al., 2009).

### 2.7. Immunofluorescence Labeling and Confocal Microscopy.

Mouse LG were processed as previously described (Meng et al., 2016; Meng et al., 2017). Briefly, mice were anesthetized by intraperitoneal injection with ketamine/xylazine (80–100 mg/kg/ 5–10 mg/kg),and euthanized by cervical dislocation. LGs were fixed, embedded in O.C.T. compound and flash frozen on dry ice. Blocks were cryosectioned at 5 μm thickness and mounted on glass slides. After being quenched and permeabilized as described (Meng et al., 2016), tissue sections were blocked with 1% BSA followed by incubation with primary and secondary antibodies. Finally, samples were mounted with ProLong anti-fade mounting medium and imaged using a ZEISS LSM 800 confocal microscope equipped with an Airyscan detector (Zeiss, Thornwood, NY). Quantification of the signal intensity was done with ImageJ (1.49V, http://imagej.nih.gov/ij/; provided in the public domain by the National Institutes of Health, Bethesda, MD, USA). For quantification of Rab3D distribution, the drawing tool was used to delineate the cell boundary and the apical half of the cells. The fluorescence intensity within the apical half and the whole cell was measured and the apical/total ratio of fluorescence intensity was calculated. Calculations were made in multiple acinar cells from 15 fields each from n=3 mouse strain and age. For quantification of α-smooth muscle actin (SMA) staining, SMA and DAPI intensity from 3 images per mouse LG per strain and age were calculated using Image J. The fluorescence intensity for each stain was measured as the Integrated Density over the entire image. For SMA staining, background fluorescence was removed using the "subtract background" toll using a rolling ball diameter=10. The intensity of SMA staining was normalized using DAPI staining.

### 2.8. Histology Analysis of LG.

Quantification of lymphocytic inflammation in LG was performed as described previously (Shah et al., 2013). Briefly, mice were euthanized and LGs were removed and fixed in 10% neutral buffer formalin prior to embedding in paraffin blocks. Paraffin sections were stained with hematoxylin-eosin (H&E) according to standard procedures and photographed using a Nikon 80i microscope (Melville, NY, USA) equipped with a digital camera. Images of three

nonconsecutive whole gland cross sections were obtained for each LG. The area of the LG occupied by lymphocytic foci was calculated using ImageJ software by a blinded examiner.

### 2.9. Statistics.

All statistical analyses were performed using GraphPad Prism software (GraphPad, San Diego, CA, USA). Shapiro Wilk, KS, and D'Agostino & Pearson omnibus normality tests were used to test for normal distribution in each data set. For normally distributed data, a one-way ANOVA with the Tukey's HSD test was used to compare differences between groups, whereas the Mann-Whitney test was used for nonparametric analysis. A $p < 0.05$ was considered as a significant difference.

## 3. Results

### 3.1. Blood glucose levels do not significantly differ in male NOD and NOR mice up to 20 weeks of age.

The male NOD is less prone to diabetes than its female counterpart, but it has been reported that 20%−30% of male NOD spontaneously develop diabetes by 30 weeks of age (Bach, 1994). In this study, at ages commonly associated with evaluation of symptoms of autoimmune dacryoadenitis in this model, none of the strains exhibited peripheral blood glucose levels over 250 mg/dL, indicative of diabetes. Furthermore, there were no significant differences in peripheral blood glucose levels between BALB/c, NOD and NOR mice at the ages measured from 10 to 20 weeks, suggesting that the male NOD mice as well as the NOR mice are relatively diabetes-free at ages below 20 weeks (Fig 1).

### 3.2. Reduction of stimulated tear flow and increased LG lymphocytic infiltration show different patterns in male NOD relative to male NOR mice.

Male NOD mice exhibit many SS-like manifestations including lymphocytic infiltration of the LG in conjunction with LG dysfunction and reduced tear flow (Doyle et al., 2007; Lavoie et al., 2011; Park et al., 2015). The same disease characteristics have also been demonstrated in the male NOR mice (Aluri et al., 2015). Here, we found no significant difference in basal tear secretion measured using phenol red threads in male BALB/c, NOD or NOR mice at ages from 10 to 20 weeks of age (Fig 2A). However, the stimulated tear volume (which was assessed only at 12 and 20 weeks of age since the procedure is terminal) showed that at 12 weeks, NOD mice had significantly lower stimulated tear volume than BALB/c (3.2 ± 0.6 μL versus 4.7 ± 0.8 μL), while there was no significant difference between BALB/c and NOR mice although a trend to decreased secretion was noted at 12 weeks (4.0 ± 1.2 μL). By 20 weeks of age, both NOD (3.0 ± 0.6 μL) and NOR (3.3 ± 0.7 μL) mice exhibited significantly lower stimulated tear volume than BALB/c mice (5.4 ± 0.6 μL) that was relatively indistinguishable (Fig 2B).

Lymphocytic infiltration was similarly assessed at 12 and 20 weeks of age by quantification, in H&E-stained LG sections, of the percentage area per cross section of the gland covered by lymphocytic foci. At 12 weeks, the percentages of LG area infiltrated by lymphocytes in male NOD mice (10.8 ± 5.4%) and NOR mice (4.8 ± 3.3%,) were significantly higher than in male BALB/c mice, while the lymphocytic infiltration was further enhanced by 20 weeks

of age in male NOD (17.5 ± 11.0%) and NOR (8.9 ± 6.1%) mice. At both ages, the extent of lymphocytic infiltration in the NOD mice was significantly greater than that measured in the NOR mice, however. In this study, BALB/c mice showed no detectable LG lymphocytic infiltration at either age (Fig 3) although previous studies have shown low levels of lymphocytic infiltration (Li et al., 2010; Schenke-Layland et al., 2010).

### 3.3. CTSS activity and expression is increased in male NOD and NOR mice compared with BALB/c mice.

Previously, our laboratory has demonstrated that CTSS activity in male NOD mouse tear fluid was significantly increased when compared with age-matched BALB/c controls (Li et al., 2010). We have further demonstrated that CTSS activity is significantly elevated in tears of SS patients relative to healthy controls, to patients with non-SS dry eye and to patients with other autoimmune diseases, suggesting that the increased tear CTSS activity might serve as a potential biomarker for diagnosis of SS (Hamm-Alvarez et al., 2014). Significantly increased CTSS activity in stimulated tears was detected from male NOD and NOR mice compared with BALB/c mice at both 12 weeks and 20 weeks of age (Fig 4A). Besides CTSS activity in tears, CTSS gene expression levels were examined in LG of male BALB/c, NOD and NOR mice. At 12 weeks and 20 weeks, NOD mouse LG showed a 7.6-fold ($p<0.001$) and 8.8fold ($p<0.05$) increase in CTSS gene expression compare to BALB/c; however, no difference in CTSS gene expression was detected between NOR and BALB/c mouse LG (Fig 4B). LG CTSS protein levels were also investigated by immunofluorescence labeling and confocal microscopy. A strong increase in CTSS immunofluorescence was observed in NOD mouse LG compared with BALB/c mouse LG, while the CTSS immunofluorescence labeling in the NOR mouse LG was less striking (Fig 4C). However, CTSS immunofluorescence was also noticeably increased in NOR mouse LG relative to BALB/c mouse LG mice, even if not as abundant as in the NOD mice. Arrows in images for NOD and NOR mice point to subapical accumulations of CTSS which our previous studies suggest may represent CTSS that reaches the tears through missorting into conventional secretory pathways or through upregulation of unconventional secretory mechanisms (Meng et al., 2016). These stores are not present in BALB/c mouse LG.

### 3.4. Expression of inflammation-related genes is elevated in NOD but not NOR mouse LG.

In addition to CTSS, gene expression levels of MHC II, a key molecule involved in antigen presentation (Villadangos et al., 1999), was also tested by RT-qPCR. Similar to the changes in gene expression of CTSS, there were large increases in gene expression of MHC II in NOD mouse LG at 12 weeks and 20 weeks of 58.42-fold ($P<0.001$) and 94.87-fold ($P=0.07$) relative to BALB/c mouse LG but no significant changes in NOR mouse LG relative to levels in age-matched BALB/c mouse LG (Fig 5A). IFN-$\gamma$ has been implicated in the development of ocular symptoms in LG and ocular surface in SS (Brookes et al., 1995; Meng et al., 2017; Willeke et al., 2009). Its gene expression level was significantly increased in the NOD mouse LG compared with BALB/c mouse LG at both 12 weeks of age (3.29-fold, $p<0.05$) and 20 weeks of age (15.25-fold, $p<0.05$)(Fig 5B). However, this cytokine was also not elevated in LG of NOR mice relative to BALB/c mice at either time point.

### 3.5. The cellular distribution of Rab3D is altered in male NOD and NOR mouse LG relative to BALB/c mouse LG.

We have previously shown that there is a significant depletion in apical stores of Rab3D and a redistribution of immunofluorescence associated with this protein to the basal domain in LG acinar cells (LGAC) of NOD mice relative to LGAC from BALB/c mice (Meng et al., 2016). In LGAC from both NOD and NOR LG, depletion of subapical Rab3D immunofluorescence and relocalization of some Rab3D immunofluorescence to the basal domain (Fig 6A, arrows) could be detected compared to its largely subapical localization beneath the lumenal actin in BALB/c mouse LGAC. Quantitative analysis of the percentage of total Rab3D immunofluorescence in the apical half of the cell in LGAC from different mouse strains showed an equivalent 50% loss of subapical Rab3D stores in LGAC from NOD and NOR mouse LG at 12 and 20 weeks (Fig 6B).

### 3.6 Myoepithelial cell thining was observed in both NOD and NOR.

Myoepithelial cells (MEC) are stellate-shaped cells with long slender processes that form a basket-like network around LGAC. These cells express α-smooth muscle actin (SMA), a marker for MECs, which can contract and thereby assist the secretory function of exocrine glands (Avci et al., 2012; Dartt, 2009; Gudjonsson et al., 2005). MECs express abundant neurotransmitter receptors such as muscarinic receptors, suggesting that these cells are responsive to the same neural stimulation responsible for inducing secretion of LG fluid (Lemullois et al., 1996). It is also likely that an important role of MEC is to support and maintain the structure of the LG (Aluri et al., 2015). Quantitative immunostaining of SMA was utilized to evaluate the relative abundance of MECs in the LG of these mice. At 12 weeks, LG from NOD and NOR mice showed significantly reduced intensities of SMA labeling compared with BALB/c mice, suggestive of a parallel degeneration or thinning of MECs. However, at 20 weeks of age, no significant differences in SMA staining could be detected between BALB/c and NOR, and BALB/c and NOD, while a statistically significant decrease was detected in SMA labeling intensity in NOD versus NOR. This suggests that MEC loss may be an early disease hallmark, and further that MEC regeneration may be responsive to the local environment including increased levels of pro-inflammatory cytokines.

## 4. Discussion

Despite difference in the immune system between human and mouse (Mestas and Hughes, 2004), murine models are invaluable tools for studying inflammatory disease pathology including elucidation of the pathological mechanisms of SS. These models provide the opportunity to observe biological changes at the tissue and molecular levels during the early disease state as well as to study disease progression in detail, a feat difficult to achieve in human patients, but essential for the development of new diagnostic and therapeutic strategies. Accumulation of new mutations by inbreeding can produce significant substrain divergence over time, and potentially, differences in substrain characteristics (De Riva et al., 2013). Phenotypic differences and genetic drift between and within NOD substrains have been observed (De Riva et al., 2013; Simecek et al., 2015) which may be due to environmental factors including the role that the gut microbiome plays in priming T cell

immunoreactions (Markle et al., 2013a; Markle et al., 2013b) which may represent an essential part of the development of autoimmunity in SS (de Paiva et al., 2016). In addtion, no consensus has been reached about onset of diabetes in male NOD mice, probably due to the divergence of different substrains housed in different environments (Bach, 1994; Kikutani and Makino, 1992). Within the NOD/ShiLtJ substrain that we used here, we consistently observed significant variance among individual mice with respect to LG lymphocytic infiltration that is reflected in Fig 3. In comparison, NOR mice exhibited less variance in this measure which may be an indicator of a more stable phenotype, albeit showing lesser lymphocytic infiltration. As for the onset of diabetes, we did not detect any significant increase in blood glucose levels as late as 20 weeks in either NOD or NOR mice compared with BALB/c mice. However, we did not perform the more sensitive diagnostic measurements such as oral glucose tolerance tests or HbA1c analysis, instead acquiring random normal range blood glucose levels.

Overall assessment of the features of LG dysfunction measured here in NOD and NOR mice suggest relatively parallel onset of the following symptoms: decreased stimulated tear secretion, increased tear CTSS activity, increased subapical CTSS immunofluorescence, redistribution of Rab3D to the basal pole of the cell, and early thinning of MECs. Our assessment suggests a relatively distinct pattern of other indicators of disease including gene expression of MHC II, IFN-$\gamma$, and CTSS, which were significantly elevated in NOD mouse LG at 12 and 20 weeks but not in NOR mouse LG. Finally, our assessment showed that the onset of lymphocytic infiltration in the LG was similar in both NOD and NOR mice but that the extent of infiltration in NOD mice was twice that in NOR mice at both ages. It is possible that the increased gene expression of pro-inflammatory factors creates an environment in which generalized inflammatory processes are exascerbated in the NOD mouse background, relative to the NOR mouse.

Previous microarray analyses in LG of male NOD mice identified CTSS as a possible tear biomarker for SS (Li et al., 2010) findings that were reinforced in a clinical study of SS patients relative to patients with other autoimmune diseases and patients with dry eye due to other causes (Hamm-Alvarez et al., 2014). Although we have not been able to investigate the source of increased tear CTSS activity in LG of SS patients at the molecular level, we have linked increased CTSS secretion to decreased Rab3D activity and to its mislocalization in LGAC in mouse models (Meng et al., 2016). While we detected upregulation of CTSS both at the gene expression level and protein level as well as elevated CTSS activity in tears in NOD mice relative to BALB/c mice, in NOR mice we detected only increased tear CTSS activity without any concomitant increased gene expression and with only modestly increased cellular CTSS protein as assessed by immunofluorescence. However we could detect increased subapical CTSS stores in LGAC of NOR mice that may contribute to the increased secreted CTSS activity. Other mechanisms may also be involved in the activation of CTSS released into tears in the NOR and NOD mice, which may include reduced expression/functionality of CTSS activity inhibitors such as cystatin C in tears (Riese et al., 1998; Saegusa et al., 2002), altered tear pH and/or enhanced proenzyme activation processes in the tears associated with protease inhibitor imbalance.

However, a unifying factor shared by both NOD and NOR mice in exhibiting increased tear CTSS seems to be mislocalization of Rab3D, occurring to the same extent and within the same time frame, suggesting that this process may be instrumental in initiating some of the changes in protein composition and loss of tear quality noted in the tears of SS patients. Interestingly, comparable changes have been observed in exocrine glands of SS patients (Bahamondes et al., 2011; Kamoi et al., 2012). Rab3D, a member of the Rab protein family, is associated with mature secretory granules or secretory vesicles in diverse cell types including those of neural, endocrine, exocrine, and immune origin (Fukuda, 2008). Because of its localization on secretory granules and its redistribution upon stimulated secretion in a number of exocrine cells including LGAC (Chen et al., 2002; Lemp, 2005), Rab3D is thought to play a key role during regulated exocytosis in exocrine secretion.

Previously we demonstrated using in vitro studies in cultured LGAC that IFN-γ exposure reduced Rab3D gene expression levels and increased CTSS secretion (Meng et al., 2017). While we have reconfirmed the significant upregulation of IFN-γ in the LG of NOD mice, in comparison, no statistically significant increase in gene expression of IFN-γ was detected in NOR mice relative to BALB/c mice, despite the relatively parallel increases in CTSS secretion and redistribution of Rab3D. This suggests that the changes in the secretory pathway and composition of the tears seen in vivo in these mice may be elicited by other factors than pro-inflammatory cytokines such as IFN-γ. One possible mechanism could be the hypofunction of the bHLH transcription factor, MIST1, which is a developmentally regulated and highly cell lineage-specific transcription factor in diverse tissues. MIST1 binds to highly conserved CATATG Eboxes to directly activate transcription of RAB3D, thus affecting the secretory phenotype of exocrine cells (Pin et al., 2000; Tian et al., 2010) The evidence that Mist1 knockout mice exhibit cellular disorganization and functional defects in the exocrine pancreas also suggests a crucial role for MIST1 in regulating exocytosis in exocrine cells (Kowalik et al., 2007). However, little is know about the expression level and functionality of MIST1 in NOD and NOR mice, nor the relationship between autoimmune inflammation and MIST1 expression.

Reduced stimulated tear production was equivalent in both NOD and NOR by 20 weeks and was decreased in NOD at 12 weeks with a trend to a decrease in the NOR mice also at 12 weeks. This reduction is associated with notable loss of SMA in MEC at both timepoints in these mice. It is also associated with a significant increase in lymphocytic infiltration of the LG at both time points. It is intriguing, however, that the extent of lymphocytic infiltration, which was greater in NOD mouse LG than in NOR mouse LG, was not correlated with either basal tear secretion (which was unchanged) nor carbachol-stimulated tear secretion (which was equivalently reduced by 20 weeks of age). This may suggest that secretory dysfunction is largely driven by other causes such as altered intracellular trafficking including redistribution of Rab3D (Meng et al., 2016), decreased neurological responsiveness (Waterman et al., 2000), loss of extracellular matrix (Li et al., 2010), and/or loss of MEC (Nashida et al., 2013). It is also possible that lymphocytic infiltration above a certain threshold in the LG is sufficient to create an environment that allows or enhances other changes required for secretory dysfunction to occur, and that more inflammation of the LG does not necessarily denote more severe SS-like disease. This is a critical issue, since

many drug development studies rely on analyses of lymphocytic infiltration of LG and SG as a key endpoint indicative of therapeutic effect.

MEC loss, as extrapolated the from loss of SMA labeling, was noted at 12 weeks in both NOD and NOR mouse LG. It is intriguing that there was an apparent restoration of MEC by 20 weeks after the initial loss at 12 weeks (Fig. 7). Studies have shown that MEC retains proliferative potential in adult uninjured LG and salivary glands (Shatos et al., 2012) and can proliferate shortly after glandular injury as a part of the restoration process (Burgess et al., 1996). With some variability across sections, it appeared that the recovery was more robust in NOR than in NOD mice, leading to the speculation that this more robust regeneration could be related to the reduced levels of pro-inflammatory cytokines and reduced lymphocytic infiltration in the NOR mice relative to the NOD. It is also worth noting that MEC are hypothesized to represent progenitor or stem cells for both LGAC and MEC. The NOR disease model may therefore represent a model of autoimmune LG injury capable of regenerative responses, in the absence of elevated pro-inflammatory cytokines that may suppress regenerative and responses like MEC proliferation such as in the NOD model.

In conclusion, in this study, we compared two commonly-used spontaneous mouse models for SS-related autoimmune dacryoadenitis that are genetically related at both the molecular and functional levels, relative to male BALB/c healthy control mice. Male NOD and NOR mice exhibited parallel development of many key features of disease including reduced stimulated tear production, increased lymphocytic infiltration of LGs, increased tear CTSS activity, increased redistribution of Rab3D to the basal pole of LGAC and early loss of MEC. Although lymphocytic infiltration occurred on a parallel time course, it was more pronounced in the NOD mouse relative to NOR, while other indicators of disease were present to approximately the same extent in both strains. Other features which have been previously associated with disease, such as increased expression of pro-inflammatory genes in the LG, were seen only in the NOD mouse.

SS is a systemic autoimmune disease with multiple contributing pathological mechanisms which include both inflammation and secretory dysfunction. In male NOD mouse LG, features of autoimmune inflammation marked by significantly increased pro-inflammatory cytokines and a more profound lymphocytic infiltration of LG, in addition to significant secretory deficits are manifested. This model is therefore useful for the study of antoimmune-related dry eye disease. In contrast, male NOR mice also manifest a major secretory deficit which is independent of the same degree of profound autoimmune inflammation, making this a model that could be advantageous to use for the study of secretory dysfunction in dry eye without the confounding effects of significant LG infiltration and elevated pro-inflammatory cytokines. Thus, the choice of the mouse model to be used from these two in future may be more rationally chosen depend upon the type of dry eye being studied and/or the specific questions being asked.

## Acknowledgements

This work was supported by NIH grants EY026635 and EY011386 and an unrestricted departmental grant from Research to Prevent Blindness. The USC School of Pharmacy Core Facility and the Research Center for Liver

Disease of Keck School of Medicine (NIH P30 DK048522) also provide help to this study. The authors thank Francie Yarber for assistance with mouse husbandry.

## Abbreviations:

| | |
|---|---|
| **CTSS** | Cathepsin S |
| **IFN-γ** | Interferon-γ |
| **LG** | lacrimal gland |
| **LGAC** | lacrimal gland acinar cell |
| **MEC** | myoepithelial cell |
| **MHC II** | major histocompatibility complex II |
| **NOD** | Non-Obese Diabetic |
| **NOR** | Non-Obese Diabetes Resistant |
| **SG** | salivary gland |
| **SMA** | α-smooth muscle actin |
| **SS** | Sjögren's Syndrome |

## References

Aluri HS, Kublin CL, Thotakura S, Armaos H, Samizadeh M, Hawley D, Thomas WM, Leavis P, Makarenkova HP, Zoukhri D, 2015 Role of Matrix Metalloproteinases 2 and 9 in Lacrimal Gland Disease in Animal Models of Sjogren's Syndrome. Investigative ophthalmology & visual science 56, 5218–5228. [PubMed: 26244298]

Aluri HS, Samizadeh M, Edman MC, Hawley DR, Armaos HL, Janga SR, Meng Z, Sendra VG, Hamrah P, Kublin CL, Hamm-Alvarez SF, Zoukhri D, 2017 Delivery of Bone Marrow-Derived Mesenchymal Stem Cells Improves Tear Production in a Mouse Model of Sjogren's Syndrome. Stem cells international 2017, 3134543. [PubMed: 28348600]

Anderson MS, Bluestone JA, 2005 The NOD mouse: a model of immune dysregulation. Annual review of immunology 23, 447–485.

Avci A, Gunhan O, Cakalagaoglu F, Gunal A, Celasun B, 2012 The cell with a thousand faces: detection of myoepithelial cells and their contributions in the cytological diagnosis of salivary gland tumors. Diagnostic cytopathology 40, 220–227. [PubMed: 20891000]

Bach JF, 1994 Insulin-dependent diabetes mellitus as an autoimmune disease. Endocrine reviews 15, 516–542. [PubMed: 7988484]

Bahamondes V, Albornoz A, Aguilera S, Alliende C, Molina C, Castro I, Urzua U, Quest AF, Barrera MJ, Gonzalez S, Sanchez M, Hartel S, Hermoso M, Leyton C, Gonzalez MJ, 2011 Changes in Rab3D expression and distribution in the acini of Sjogren's syndrome patients are associated with loss of cell polarity and secretory dysfunction. Arthritis and rheumatism 63, 3126–3135. [PubMed: 21702009]

Brookes SM, Price EJ, Venables PJ, Maini RN, 1995 Interferon-gamma and epithelial cell activation in Sjogren's syndrome. British journal of rheumatology 34, 226–231. [PubMed: 7728396]

Burgess KL, Dardick I, Cummins MM, Burford-Mason AP, Bassett R, Brown DH, 1996 Myoepithelial cells actively proliferate during atrophy of rat parotid gland. Oral surgery, oral medicine, oral pathology, oral radiology, and endodontics 82, 674–680.

Chen X, Edwards JA, Logsdon CD, Ernst SA, Williams JA, 2002 Dominant negative Rab3D inhibits amylase release from mouse pancreatic acini. The Journal of biological chemistry 277, 18002–18009. [PubMed: 11875077]

Conus S, Simon HU, 2010 Cathepsins and their involvement in immune responses. Swiss medical weekly 140, w13042. [PubMed: 20648403]

Dartt DA, 2009 Neural regulation of lacrimal gland secretory processes: relevance in dry eye diseases. Progress in retinal and eye research 28, 155–177. [PubMed: 19376264]

de Paiva CS, Jones DB, Stern ME, Bian F, Moore QL, Corbiere S, Streckfus CF, Hutchinson DS, Ajami NJ, Petrosino JF, Pflugfelder SC, 2016 Altered Mucosal Microbiome Diversity and Disease Severity in Sjogren Syndrome. Scientific reports 6, 23561. [PubMed: 27087247]

De Riva A, Varley MC, Bluck LJ, Cooke A, Deery MJ, Busch R, 2013 Accelerated turnover of MHC class II molecules in nonobese diabetic mice is developmentally and environmentally regulated in vivo and dispensable for autoimmunity. Journal of immunology (Baltimore, Md. : 1950) 190, 5961–5971.

Doyle ME, Boggs L, Attia R, Cooper LR, Saban DR, Nguyen CQ, Peck AB, 2007 Autoimmune dacryoadenitis of NOD/LtJ mice and its subsequent effects on tear protein composition. The American journal of pathology 171, 1224–1236. [PubMed: 17823290]

Evans E, Zhang W, Jerdeva G, Chen CY, Chen X, Hamm-Alvarez SF, Okamoto CT, 2008 Direct interaction between Rab3D and the polymeric immunoglobulin receptor and trafficking through regulated secretory vesicles in lacrimal gland acinar cells. American journal of physiology. Cell physiology 294, C662–674. [PubMed: 18171724]

Fukuda M, 2008 Regulation of secretory vesicle traffic by Rab small GTPases. Cellular and molecular life sciences : CMLS 65, 2801–2813. [PubMed: 18726178]

Gudjonsson T, Adriance MC, Sternlicht MD, Petersen OW, Bissell MJ, 2005 Myoepithelial cells: their origin and function in breast morphogenesis and neoplasia. Journal of mammary gland biology and neoplasia 10, 261–272. [PubMed: 16807805]

Hamm-Alvarez SF, Janga SR, Edman MC, Madrigal S, Shah M, Frousiakis SE, Renduchintala K, Zhu J, Bricel S, Silka K, Bach D, Heur M, Christianakis S, Arkfeld DG, Irvine J, Mack WJ, Stohl W, 2014 Tear cathepsin S as a candidate biomarker for Sjogren's syndrome. Arthritis Rheumatol 66, 1872–1881. [PubMed: 24644101]

Hu Y, Nakagawa Y, Purushotham KR, Humphreys-Beher MG, 1992 Functional changes in salivary glands of autoimmune disease-prone NOD mice. The American journal of physiology 263, E607–614. [PubMed: 1415679]

Humphreys-Beher MG, 1996 Animal models for autoimmune disease-associated xerostomia and xerophthalmia. Advances in dental research 10, 73–75. [PubMed: 8934930]

Kamoi M, Ogawa Y, Nakamura S, Dogru M, Nagai T, Obata H, Ito M, Kaido M, Kawakita T, Okada Y, Kawakami Y, Shimmura S, Tsubota K, 2012 Accumulation of secretory vesicles in the lacrimal gland epithelia is related to non-Sjogren's type dry eye in visual display terminal users. PloS one 7, e43688. [PubMed: 22962587]

Kikutani H, Makino S, 1992 The murine autoimmune diabetes model: NOD and related strains. Advances in immunology 51, 285–322. [PubMed: 1323922]

Kowalik AS, Johnson CL, Chadi SA, Weston JY, Fazio EN, Pin CL, 2007 Mice lacking the transcription factor Mist1 exhibit an altered stress response and increased sensitivity to caerulein-induced pancreatitis. American journal of physiology. Gastrointestinal and liver physiology 292, G1123–1132. [PubMed: 17170023]

Lavoie TN, Lee BH, Nguyen CQ, 2011 Current concepts: mouse models of Sjogren's syndrome. Journal of biomedicine & biotechnology 2011, 549107. [PubMed: 21253584]

Lemp MA, 2005 Dry eye (Keratoconjunctivitis Sicca), rheumatoid arthritis, and Sjogren's syndrome. American journal of ophthalmology 140, 898–899. [PubMed: 16310468]

Lemullois M, Rossignol B, Mauduit P, 1996 Immunolocalization of myoepithelial cells in isolated acini of rat exorbital lacrimal gland: cellular distribution of muscarinic receptors. Biology of the cell 86, 175–181. [PubMed: 8893507]

Li X, Wu K, Edman M, Schenke-Layland K, MacVeigh-Aloni M, Janga SR, Schulz B, Hamm-Alvarez SF, 2010 Increased expression of cathepsins and obesity-induced pro-inflammatory cytokines in

lacrimal glands of male NOD mouse. Investigative ophthalmology & visual science 51, 5019–5029. [PubMed: 20463324]

Maciel G, Crowson CS, Matteson EL, Cornec D, 2016 Prevalence of Primary Sjogren's Syndrome in a US Population-Based Cohort. Arthritis care & research.

Many MC, Maniratunga S, Denef JF, 1996 The non-obese diabetic (NOD) mouse: an animal model for autoimmune thyroiditis. Experimental and clinical endocrinology & diabetes : official journal, German Society of Endocrinology [and] German Diabetes Association 104 Suppl 3, 17–20.

Markle JG, Frank DN, Mortin-Toth S, Robertson CE, Feazel LM, Rolle-Kampczyk U, von Bergen M, McCoy KD, Macpherson AJ, Danska JS, 2013a Sex differences in the gut microbiome drive hormone-dependent regulation of autoimmunity. Science (New York, N.Y.) 339, 1084–1088.

Markle JG, Mortin-Toth S, Wong AS, Geng L, Hayday A, Danska JS, 2013b gammadelta T cells are essential effectors of type 1 diabetes in the nonobese diabetic mouse model. Journal of immunology (Baltimore, Md. : 1950) 190, 5392–5401.

Meng Z, Edman MC, Hsueh PY, Chen CY, Klinngam W, Tolmachova T, Okamoto CT, Hamm-Alvarez SF, 2016 Imbalanced Rab3D versus Rab27 increases cathepsin S secretion from lacrimal acini in a mouse model of Sjogren's Syndrome. American journal of physiology. Cell physiology 310, C942–954. [PubMed: 27076615]

Meng Z, Klinngam W, Edman MC, Hamm-Alvarez SF, 2017 Interferon-gamma treatment in vitro elicits some of the changes in cathepsin S and antigen presentation characteristic of lacrimal glands and corneas from the NOD mouse model of Sjogren's Syndrome. PloS one 12, e0184781. [PubMed: 28902875]

Mestas J, Hughes CC, 2004 Of mice and not men: differences between mouse and human immunology. Journal of immunology (Baltimore, Md. : 1950) 172, 2731–2738.

Nashida T, Yoshie S, Haga-Tsujimura M, Imai A, Shimomura H, 2013 Atrophy of myoepithelial cells in parotid glands of diabetic mice; detection using skeletal muscle actin, a novel marker(). FEBS Open Bio 3, 130–134.

Nguyen CQ, Peck AB, 2009 Unraveling the pathophysiology of Sjogren syndrome-associated dry eye disease. The ocular surface 7, 11–27. [PubMed: 19214349]

Nocturne G, Mariette X, 2015 Sjogren Syndrome-associated lymphomas: an update on pathogenesis and management. British journal of haematology 168, 317–327. [PubMed: 25316606]

Park YS, Gauna AE, Cha S, 2015 Mouse Models of Primary Sjogren's Syndrome. Current pharmaceutical design 21, 2350–2364. [PubMed: 25777752]

Pin CL, Bonvissuto AC, Konieczny SF, 2000 Mist1 expression is a common link among serous exocrine cells exhibiting regulated exocytosis. The Anatomical record 259, 157–167. [PubMed: 10820318]

Reddy VY, Zhang QY, Weiss SJ, 1995 Pericellular mobilization of the tissue-destructive cysteine proteinases, cathepsins B, L, and S, by human monocyte-derived macrophages. Proceedings of the National Academy of Sciences of the United States of America 92, 3849–3853. [PubMed: 7731994]

Riese RJ, Mitchell RN, Villadangos JA, Shi GP, Palmer JT, Karp ER, De Sanctis GT, Ploegh HL, Chapman HA, 1998 Cathepsin S activity regulates antigen presentation and immunity. The Journal of clinical investigation 101, 2351–2363. [PubMed: 9616206]

Roescher N, Lodde BM, Vosters JL, Tak PP, Catalan MA, Illei GG, Chiorini JA, 2012 Temporal changes in salivary glands of non-obese diabetic mice as a model for Sjogren's syndrome. Oral diseases 18, 96–106. [PubMed: 21914088]

Routsias JG, Goules JD, Charalampakis G, Tzima S, Papageorgiou A, Voulgarelis M, 2013 Malignant lymphoma in primary Sjogren's syndrome: an update on the pathogenesis and treatment. Seminars in arthritis and rheumatism 43, 178–186. [PubMed: 23816048]

Saegusa K, Ishimaru N, Yanagi K, Arakaki R, Ogawa K, Saito I, Katunuma N, Hayashi Y, 2002 Cathepsin S inhibitor prevents autoantigen presentation and autoimmunity. The Journal of clinical investigation 110, 361–369. [PubMed: 12163455]

Salomon B, Rhee L, Bour-Jordan H, Hsin H, Montag A, Soliven B, Arcella J, Girvin AM, Padilla J, Miller SD, Bluestone JA, 2001 Development of spontaneous autoimmune peripheral

polyneuropathy in B7–2-deficient NOD mice. The Journal of experimental medicine 194, 677–684. [PubMed: 11535635]

Schenke-Layland K, Xie J, Magnusson M, Angelis E, Li X, Wu K, Reinhardt DP, Maclellan WR, Hamm-Alvarez SF, 2010 Lymphocytic infiltration leads to degradation of lacrimal gland extracellular matrix structures in NOD mice exhibiting a Sjogren's syndrome-like exocrinopathy. Experimental eye research 90, 223–237. [PubMed: 19852957]

Shah M, Edman MC, Janga SR, Shi P, Dhandhukia J, Liu S, Louie SG, Rodgers K, Mackay JA, Hamm-Alvarez SF, 2013 A rapamycin-binding protein polymer nanoparticle shows potent therapeutic activity in suppressing autoimmune dacryoadenitis in a mouse model of Sjogren's syndrome. Journal of controlled release : official journal of the Controlled Release Society 171, 269–279. [PubMed: 23892265]

Shah M, Edman MC, Reddy Janga S, Yarber F, Meng Z, Klinngam W, Bushman J, Ma T, Liu S, Louie S, Mehta A, Ding C, MacKay JA, Hamm-Alvarez SF, 2017 Rapamycin Eye Drops Suppress Lacrimal Gland Inflammation In a Murine Model of Sjögren's Syndrome. Investigative ophthalmology & visual science 58, 372–385. [PubMed: 28122086]

Shatos MA, Haugaard-Kedstrom L, Hodges RR, Dartt DA, 2012 Isolation and Characterization of Progenitor Cells in Uninjured, Adult Rat Lacrimal Gland. Investigative ophthalmology & visual science 53, 2749–2759. [PubMed: 22427571]

Simecek P, Churchill GA, Yang H, Rowe LB, Herberg L, Serreze DV, Leiter EH, 2015 Genetic Analysis of Substrain Divergence in Non-Obese Diabetic (NOD) Mice. G3 (Bethesda, Md.) 5, 771–775.

Sisto M, Lorusso L, Ingravallo G, Tamma R, Nico B, Ribatti D, Ruggieri S, Lisi S, 2018 Reduced myofilament component in primary Sjogren's syndrome salivary gland myoepithelial cells. Journal of molecular histology 49, 111–121. [PubMed: 29302763]

Takahashi M, Ishimaru N, Yanagi K, Haneji N, Saito I, Hayashi Y, 1997 High incidence of autoimmune dacryoadenitis in male non-obese diabetic (NOD) mice depending on sex steroid. Clinical and experimental immunology 109, 555–561. [PubMed: 9328136]

Tian X, Jin RU, Bredemeyer AJ, Oates EJ, Blazewska KM, McKenna CE, Mills JC, 2010 RAB26 and RAB3D are direct transcriptional targets of MIST1 that regulate exocrine granule maturation. Molecular and cellular biology 30, 1269–1284. [PubMed: 20038531]

Tsubota K, Fujita H, Tsuzaka K, Takeuchi T, 2000 Mikulicz's disease and Sjogren's syndrome. Investigative ophthalmology & visual science 41, 1666–1673. [PubMed: 10845583]

Villadangos JA, Bryant RA, Deussing J, Driessen C, Lennon-Dumenil AM, Riese RJ, Roth W, Saftig P, Shi GP, Chapman HA, Peters C, Ploegh HL, 1999 Proteases involved in MHC class II antigen presentation. Immunological reviews 172, 109–120. [PubMed: 10631941]

Waterman SA, Gordon TP, Rischmueller M, 2000 Inhibitory effects of muscarinic receptor autoantibodies on parasympathetic neurotransmission in Sjogren's syndrome. Arthritis and rheumatism 43, 1647–1654. [PubMed: 10902771]

Willeke P, Schluter B, Schotte H, Domschke W, Gaubitz M, Becker H, 2009 Interferon-gamma is increased in patients with primary Sjogren's syndrome and Raynaud's phenomenon. Seminars in arthritis and rheumatism 39, 197–202. [PubMed: 18571695]

Wu K, Joffre C, Li X, MacVeigh-Aloni M, Hom M, Hwang J, Ding C, Gregoire S, Bretillon L, Zhong JF, Hamm-Alvarez SF, 2009 Altered expression of genes functioning in lipid homeostasis is associated with lipid deposition in NOD mouse lacrimal gland. Experimental eye research 89, 319–332. [PubMed: 19345210]

## Highlights

- Male NOD and NOR mice are common models for autoimmune-dacryoadenitis.
- Male NOD and NOR mice showed comparable changes in tear flow and tear cathepsin S
- Male NOD and NOR mice showed comparable redistributions of Rab3D and cathepsin S
- Male NOD mice showed more lymphocytic inflammation in lacrimal gland than NOR mice
- NOD but not NOR lacrimal glands had increased gene expression of MHC II and IFN-γ

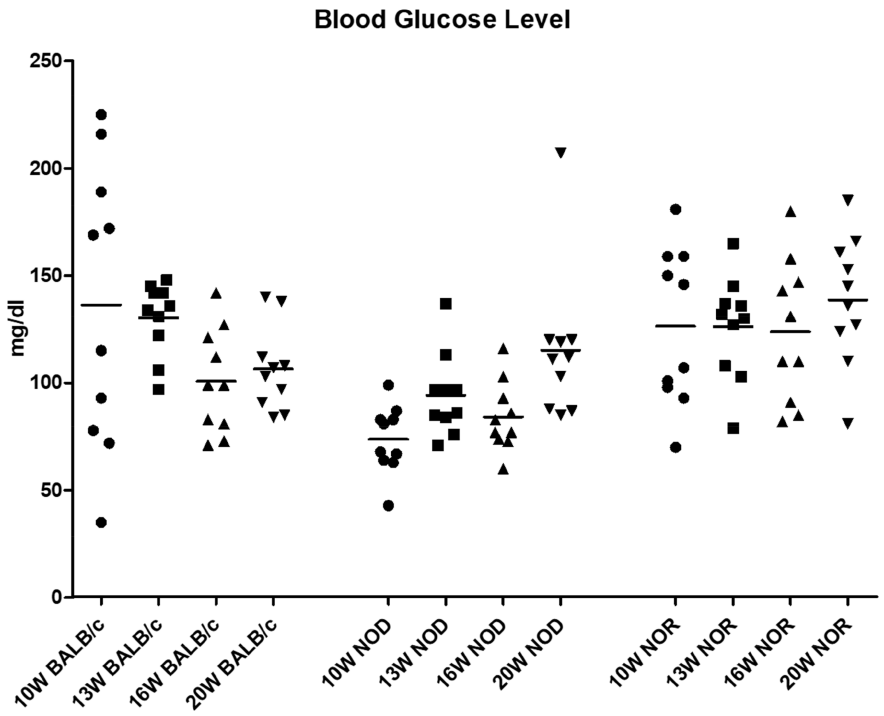


**Figure 1. Blood glucose levels in male BALB/c, NOD and NOR mice.**

Blood glucose levels of BALB/c, NOD and NOR mice at 10, 13, 16 and 20 weeks of age were measured in peripheral blood acquired by tail nick. A one-way ANOVA with the Tukey's HSD test was used to compare different time points within each strain; another one-way ANOVA with Tukey's HSD test was used to compare different strains at each measured time point. (N=10 per strain with the same mice being measured at each age).

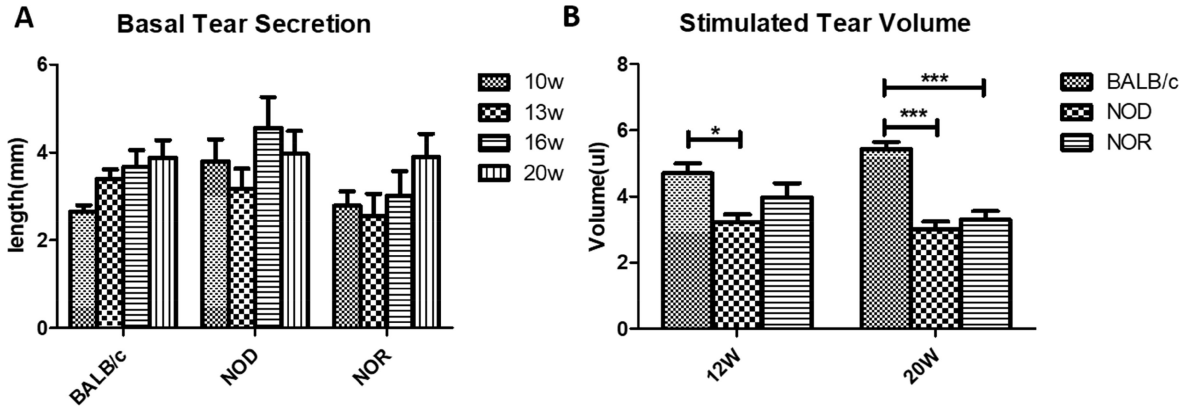


**Figure 2. Basal and Stimulated Tear Production in male BALB/c, NOD and NOR mice.**

A) Basal tear secretion in male BALB/c, NOD and NOR mice was measured using a phenol red thread test from 10 weeks of age to 20 weeks of age. A one-way ANOVA with the Tukey's HSD test was used to compare different time points within each strain; another one-way ANOVA with Tukey's HSD test was used to compare different strains at each measured time point. (N=10 mice per strain with the same mice measured at each age). B) Carbachol-stimulated tear volume was measured in male BALB/c, NOD and NOR mice at 12 and 20 weeks of age with mice under general anesthesia. A one-way ANOVA with the Tukey's HSD test was used across strains at each time point. (N=7 per strain per age) (*P ≤ 0.05; **P ≤ 0.01; ***P ≤ 0.001).

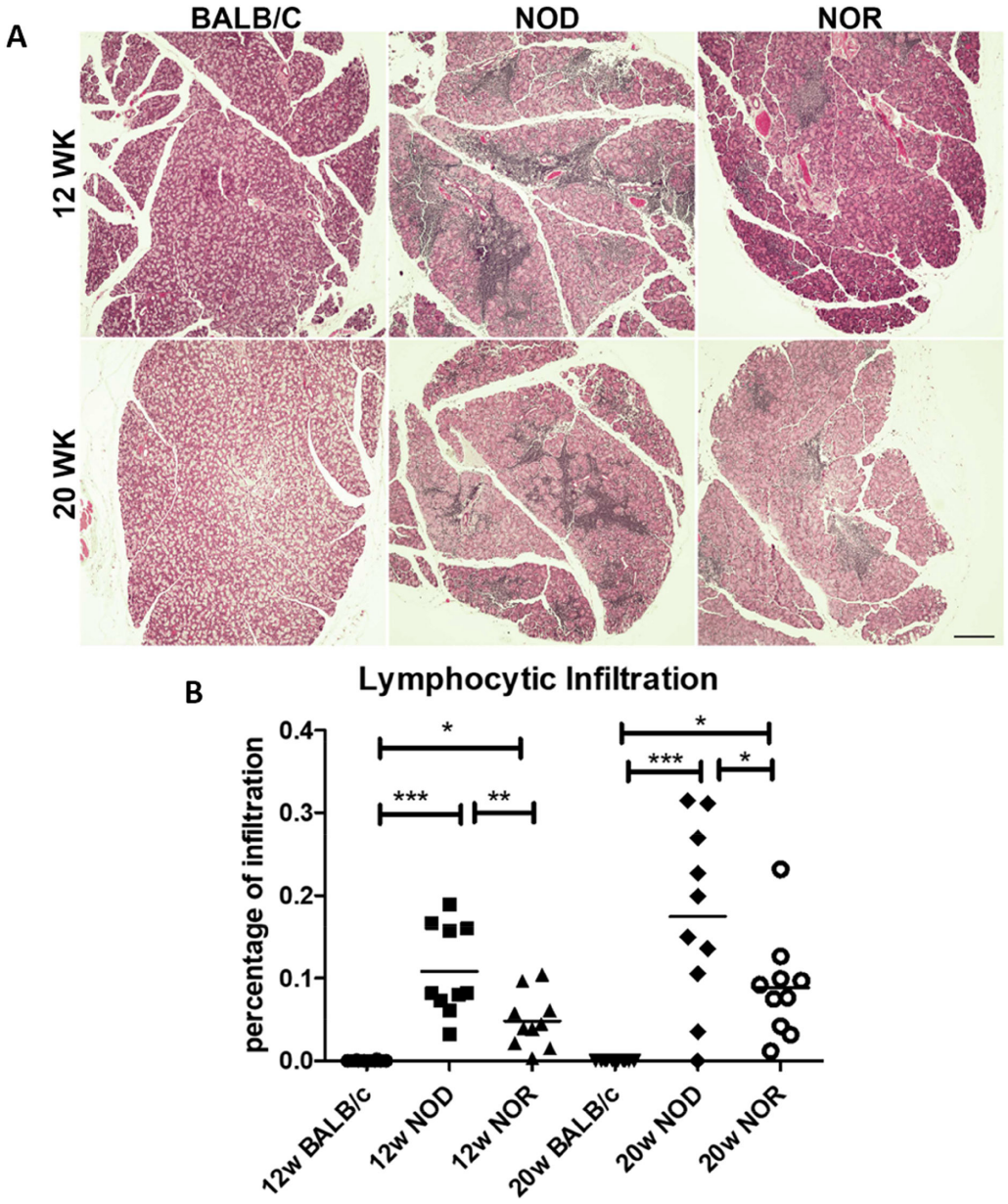


**Figure 3. LG lymphocytic Infiltration in BALB/c, NOD and NOR mice.**

A) Representative images of H&E staining in male NOD, NOR and BALB/c mouse LG at 12 and 20 weeks of age. B) Quantification of the percentage of lymphocytic infiltration in multiple sections from each LG as described in Methods. A one-way ANOVA with the Tukey's HSD test was used across strains at each time point. Scale bar=200 μm (N=10 mice per strain and age) (*P ≤ 0.05; **P ≤ 0.01; ***P ≤ 0.001).

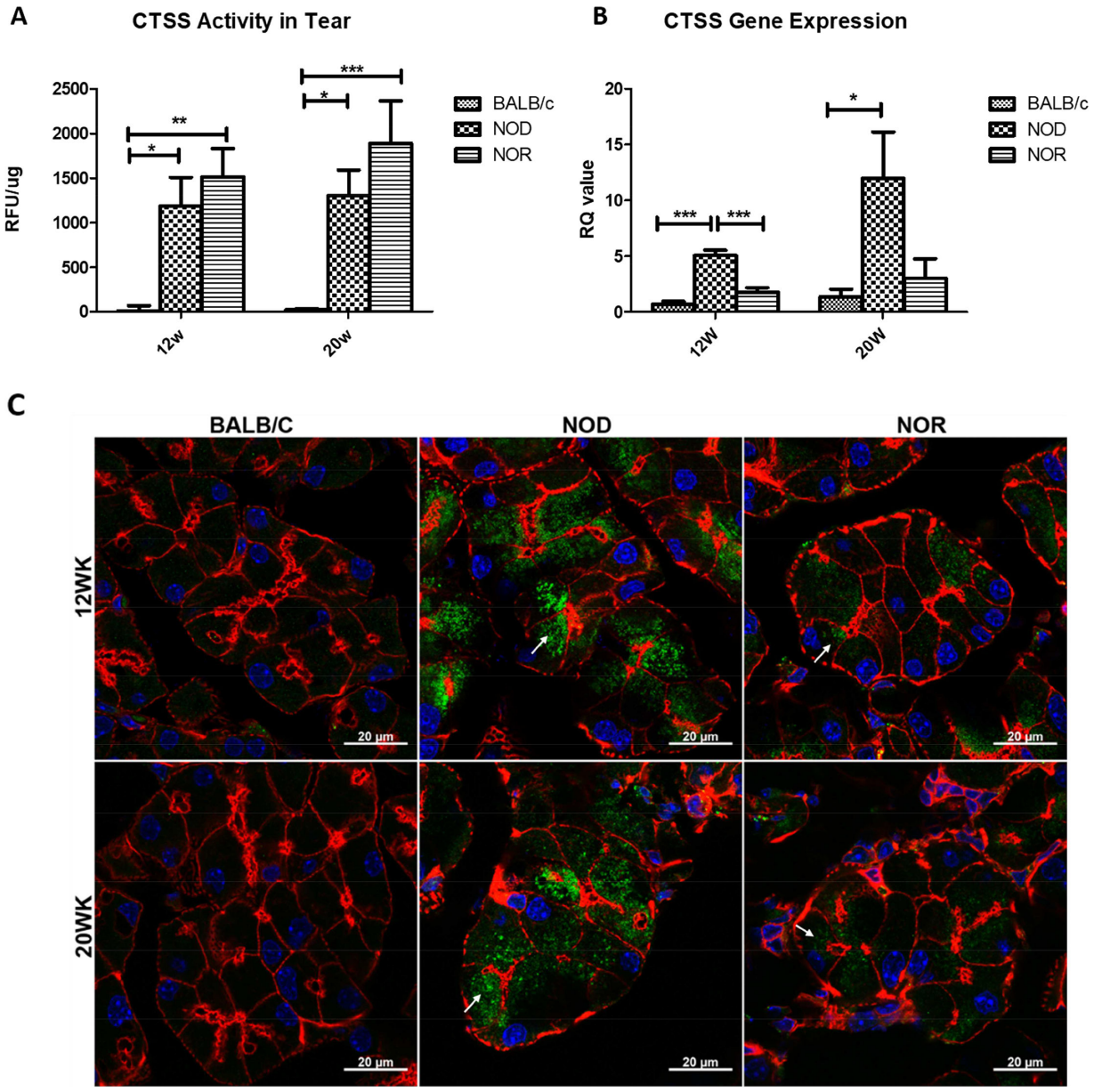


**Figure 4. CTSS activity in stimulated tears and its expression and distribution levels in LG of male BALB/c, NOD and NOR mice.**

A) CTSS activity levels in carbachol-stimulated tears from male BALB/c, NOD and NOR mice was measured at 12 and 20 weeks of age. A one-way ANOVA with the Tukey's HSD test was used across the strains at each time point. (N=7). B) Gene expression levels for LG CTSS in male BALB/c, NOD and NOR mice were measured at 12 and 20 weeks. A one-way ANOVA with Tukey's HSD test was used across strains at each time point. (N=5) (*P ≤ 0.05; **P ≤ 0.01; ***P ≤ 0.001). C) Intracellular distribution of CTSS protein in LG of male BALB/c, NOD and NOR mice at 12 and 20 weeks of age was evaluated by immunofluorescence labeling. Green: CTSS. Red: Actin. Blue: DAPI. Scale bar, 20 μm. Results shown are typical of those seen from multiple images taken from LG from n=3 mice of each type in each age group.

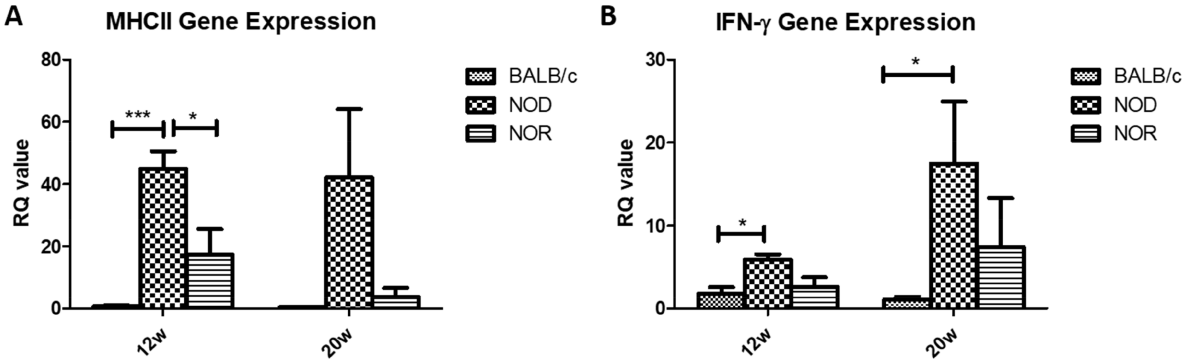


**Figure 5. Expression of inflammation-related genes in LG of NOD and NOR mouse relative to age-matched BALB/c mouse LG.**

Gene expression levels of MHC II (A) and IFN-γ (B) were measured by RT-PCR in LG from male BALB/c, NOD and NOR mice at 12 and 20 weeks of age. A one-way ANOVA with Tukey's HSD test was used across strains at each time point. (N=5 per strain per age) (*P ≤ 0.05; **P ≤ 0.01; ***P ≤ 0.001).

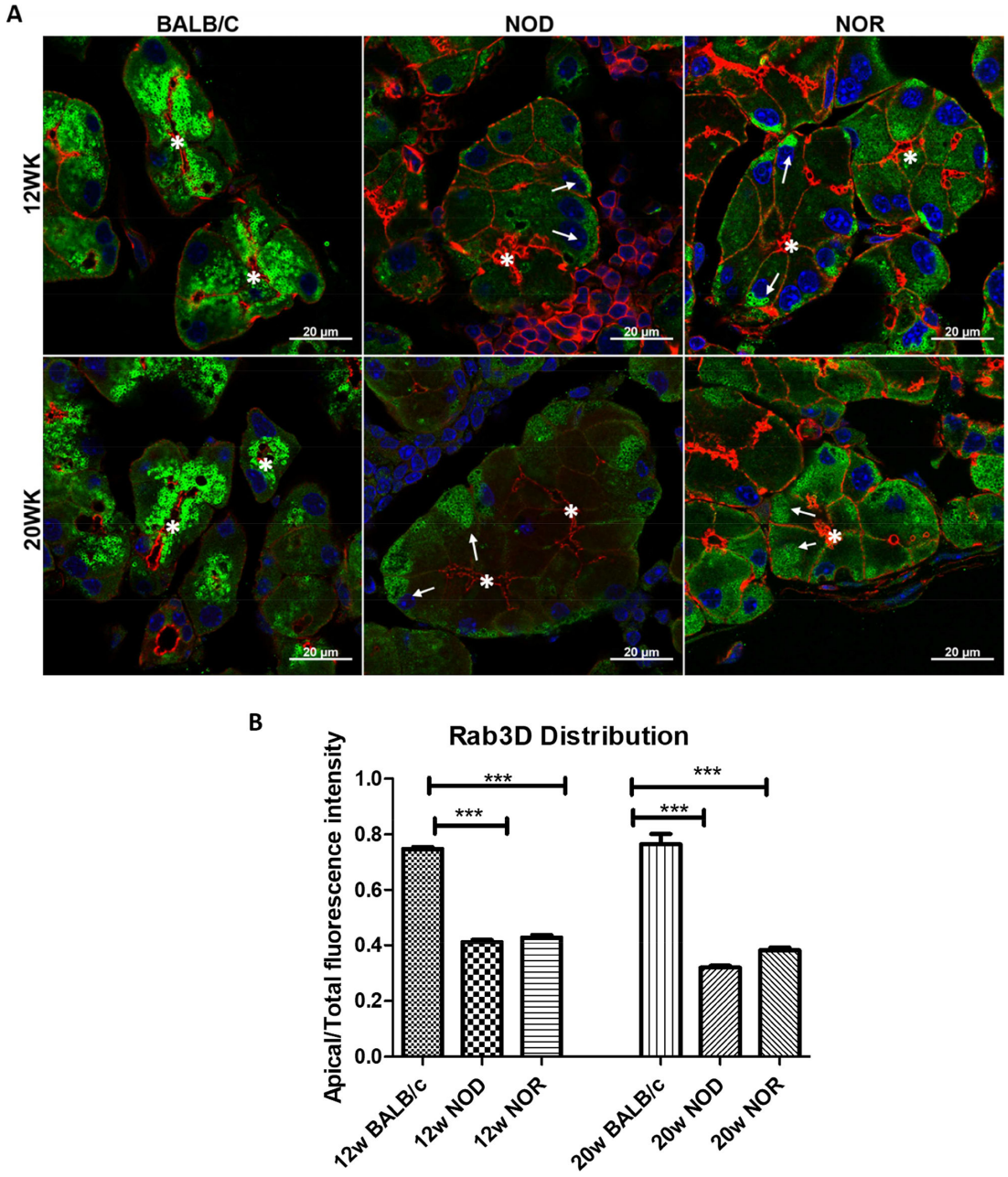


**Figure 6. Relative distributions of Rab3D in LG of male BALB/c, NOD and NOR mice at 12 and 20 weeks of age.**

A) The distribution of Rab3D vesicles in LGAC in BALB/c, NOD and NOR mice was assessed by immunofluorescence. Green: Rab3D. Red: Actin. Blue: DAPI. Asterisk: Lumenal region. Arrows: Basal redistribution of Rab3D vesicles. Scale bar, 20 μm. Results shown are typical of multiple images taken from LG from n=3 mice per strain per age. B) Quantification of subapical Rab3D vesicle accumulation in LGAC from BALB/c, NOD and NOR mice. A one-way ANOVA with Tukey's HSD test was used across strains at each time point. (N=15 acini per mouse, 3 mice per strain per age) (*P ≤ 0.05;**P ≤ 0.01;***P ≤ 0.001).

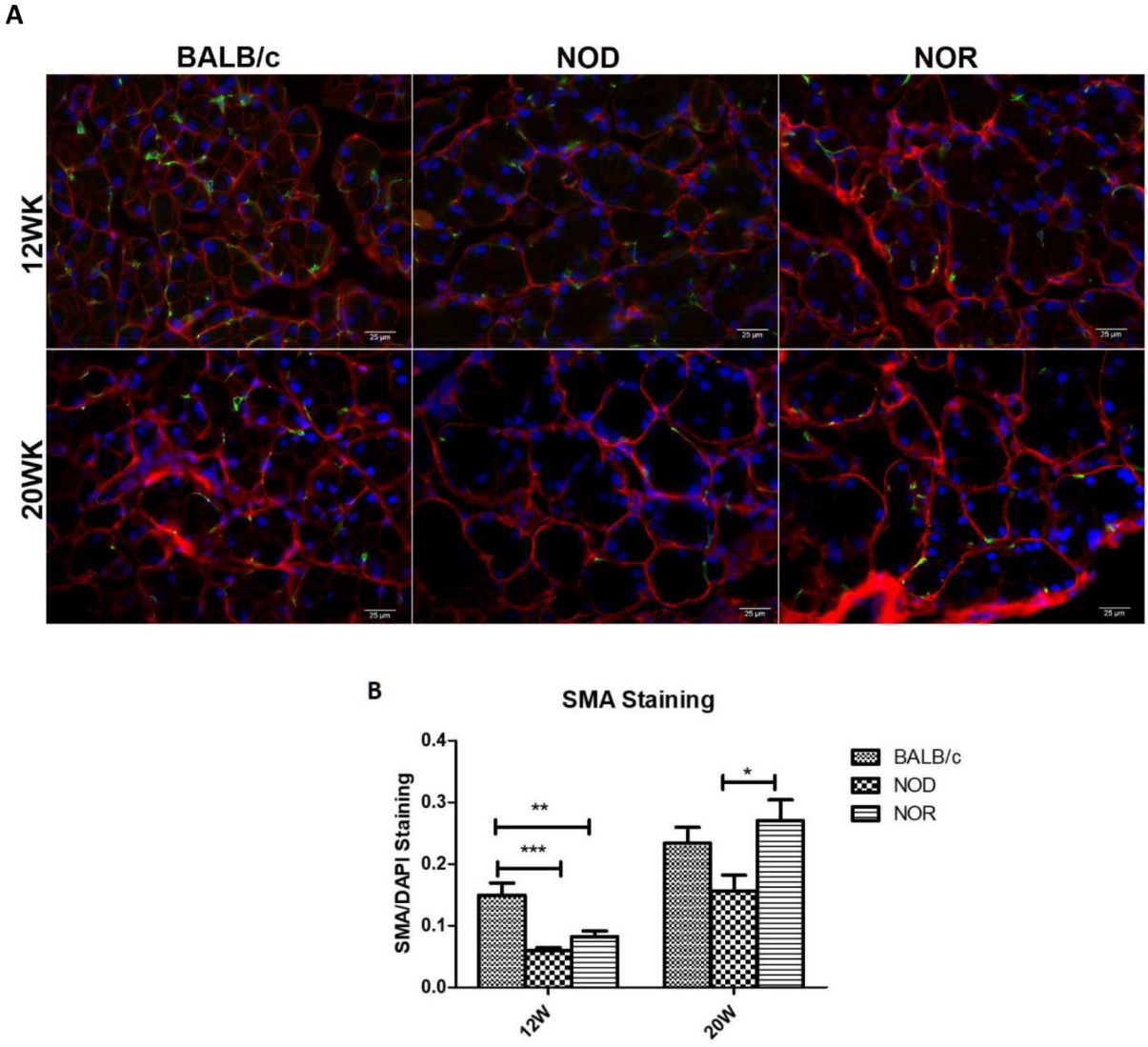


**Figure 7. SMA-enriched MEC distribution in NOD and NOR mouse LG relative to age-matched BALB/c mouse LG.**

A) Immunofluorescence labeling of alpha-SMA (green), a marker for MEC, in LG at 12 and 20 weeks of age. Red: E-Cadherin. Blue: DAPI. Results shown are representative of multiple images taken from LG of n=3 mice per strain and age. Scale bar, 25 μm. B) Quantification of integrated density of alpha-SMA staining normalized to DAPI staining. A one-way ANOVA with Tukey's HSD test was used across strains at each time point. (N=3 pictures per mouse, 3 mice per strain per age) (*$P \leq 0.05$;**$P \leq 0.01$;***$P \leq 0.001$).